Crystal Structure, Low-Temperature Heat Capacities, and Thermodynamic Properties of Bis(dodecylammonium) Tetrachlorocuprate $(C_{12}H_{28}N)_2CuCl_4(s)$

Dong-Hua He, You-Ying Di,* Yao Yao, Yu-Pu Liu, and Wen-Yan Dan

College of Chemistry and Chemical Engineering, Liaocheng University, Liaocheng 252059, Shandong, People's Republic of China

Crystalline bis(dodecylammonium) tetrachlorocuprate $(C_{12}H_{28}N)_2CuCl_4(s)$ was synthesized. Chemical analysis, elemental analysis, and X-ray crystallography were applied to characterize the composition and crystal structure of the compound. The lattice potential energy (U_{POT}) of the title compound was calculated to be 862.56 kJ·mol^{-1}. Low-temperature heat capacities of the compound were measured by a precision automatic adiabatic calorimeter over the temperature range from (78 to 390) K. Two continuous solid−solid phase transitions were observed. The temperatures, molar enthalpies, and entropies of the two phase transitions were determined to be: $T_{trs,1}$ = (329.03 ± 0.24) K, $\Delta_{trs}H_{m,1}$ = (64.24 ± 0.35) kJ·mol^{-1}, $\Delta_{trs}S_{m,1}$ = (194.57 ± 1.09) J·K^{-1}·mol^{-1}, $T_{trs,2}$ = (336.98 ± 0.18) K, $\Delta_{trs}H_{m,2}$ = (20.81 ± 0.30) kJ·mol^{-1}, and $\Delta_{trs}S_{m,2}$ = (61.75 ± 0.87) J·K^{-1}·mol^{-1}, respectively. Two polynomial equations of heat capacity against the reduced temperature in the region of (78 to 311) K and (340 to 390) K were fitted by a least-squares method. On the basis of the two polynomials, the smoothed heat capacities and thermodynamic functions of the compound relative to the standard reference temperature of 298.15 K were calculated and tabulated with an interval of 5 K. In addition, two solid−solid phase transitions and a melting process of the title compound were verified by the differential scanning calorimetry (DSC) technique.

Introduction

Energy is one of the most basic driving forces for societal development and economic growth and the basis of human survival. Nowadays, with the development of society, the demand of human beings for energy is ever-growing, but the supply of the energy always falls short of demand. Therefore, the development of new green energy, improvement of the utilization rate of energy in the modern world, and reduction of waste from energy utilization have attracted much attention. For this purpose, phase change materials (PCMs), especially solid−solid phase change materials (SSPCMs), have become a hot spot in the fields of energy and material science.[1]

PCMs absorb and release large amounts of energy as latent heat at a constant phase transition temperature and thus are used for heat storage and temperature control. Latent heat storage is the most attractive due to its high storage density and small temperature variation from storage to retrieval. SSPSMs undergo a phase change from one solid to another solid provided that the operating temperature is below the phase transition temperature of the materials. They need not be capsulated, provide no corrosion, and enable quick heat transfer;[1] hence, they have a very wide range of applications. For example, they are appropriate for latent heat storage in buildings without encapsulation. Latent heat storage by using PCM for recovering waste heat from industries is also quite an attractive option.[2]

Many papers[3−6] have reported the bis(alkylammonium) tetrahalometallates(II) (n-$C_nH_{2n+1}NH_3)_2MX_4$ as a kind of SSPCM, in which M is a divalent transition metal atom, X is a halogen, and n varies between 8 and 18.

* To whom correspondence may be addressed: Prof. You-Ying Di, College of Chemistry and Chemical Engineering, Liaocheng University, Liaocheng 252059, Shandong Province, P. R. China. Fax: +86-635-8239121. E-mail: diyouying@126.com and yydi@lcu.edu.cn.

Studies on the structural phase transitions of $(C_{12}H_{28}N)_2CuCl_4$ have been undertaken by several research workers using various differential scanning calorimetry (DSC) techniques over the past year.[3,4]

Adiabatic calorimetry is an important experimental method widely used in the fields of thermochemistry and thermophysics. The technique has been widely applied to measure heat capacities of many substances owing to its high precision. Heat capacity is not only one of the most fundamental thermodynamic properties of materials and necessary for much theoretical research in physics, chemistry, and engineering technology related to materials but also characteristic data which closely links with the structure and phase transition of substances. On the basis of heat capacity measurements, thermodynamic functions, such as enthalpy, entropy, and Gibbs energy, can be derived.[7,8]

In this paper, the title compound was synthesized, and its crystal structure was characterized by X-ray crystallography. Low-temperature heat capacities of $(C_{12}H_{28}N)_2CuCl_4$ were measured by a precision automatic adiabatic calorimeter over the temperature range from (78 to 390) K. Two solid−solid phase transition processes were observed. The temperatures, molar enthalpies, and entropies of the two phase transitions were determined.

Experimental Section

Synthesis of Sample. *n*-Dodecylamine, hydrochloride acid (37 %), and copper chloride dihydrate as reactants and anhydrous methyl alcohol as the solvent were all of analytical grade. The reactants were accurately weighed at the molar ratio of n(*n*-dodecylamine)/n(hydrochloric acid)/n(copper chloride dihydrate) = 2:2:1, in which hydrochloric acid is slightly excessive and slowly dissolved in anhydrous methyl alcohol. The mixture was heated by an electric jacket and stirred under

10.1021/je100699g
Published on Web 11/15/2010

Table 1. Crystal Data and Structure Refinement for Bis(dodecylammonium) Tetrachlorocuprate

crystallographic date	structure refinement
empirical formula	$C_{24}H_{56}N_2Cl_4Cu$
formula weight	578.05
temperature	298(2) K
wavelength	0.71073 Å
crystal system	triclinic
space group	*P*-1
unit cell dimensions	$a = 7.3357(6)$ Å; $\alpha = 91.786(2)°$ $b = 7.5884(7)$ Å; $\beta = 90.9540(10)°$ $c = 31.05(3)$ Å; $\gamma = 90.0600(10)°$
volume	1727.5(14) Å^3
Z	2
calculated density	1.111 Mg·m^{-3}
absorption coefficient	0.954 mm^{-1}
F(000)	622
crystal size	0.48 × 0.47 × 0.13 mm
θ range for data collection	1.97 to 25.02°
limiting indices	$-8 \le h \le 8$, $-9 \le k \le 8$, $-33 \le l \le 36$
reflections collected/unique	8611/5916 [*R*(int) = 0.0452]
completeness to $\theta = 25.02$	97.0 %
absorption correction	semiempirical from equivalents
max. and min. transmission	0.8860 and 0.6573
refinement method	full-matrix least-squares on F^2
data/restraints/parameters	5916/336/287
goodness-of-fit on F^2	1.092
final *R* indices [$I > 2\sigma(I)$]	$R_1 = 0.1074$, $wR_2 = 0.3123$
R indices (all data)	$R_1 = 0.1446$, $wR_2 = 0.3390$
largest diff. peak and hole	1.937 and −1.064 e·Å^{-3}

Table 2. Selected Bond Lengths (Å) and Bond Angles (deg) for Bis(dodecylammonium) Tetrachlorocuprate[a]

Cu(1)−Cl(1)	2.311(2)	Cl(1)−Cu(1)−Cl(1)#1	180.00(13)
Cu(1)−Cl(1)#1	2.311(2)	Cl(1)−Cu(1)−Cl(2)#1	89.43(9)
Cu(1)−Cl(2)#1	2.329(3)	Cl(1)#1−Cu(1)−Cl(2)#1	90.57(9)
Cu(1)−Cl(2)	2.329(3)	Cl(1)−Cu(1)−Cl(2)	90.57(9)
Cu(1)−Cl(3)	3.007(2)	Cl(1)#1−Cu(1)−Cl(2)	89.43(9)
Cu(2)−Cl(3)#2	2.308(2)	Cl(2)#1−Cu(1)−Cl(2)	180.00(2)
Cu(2)−Cl(3)	2.308(2)	Cl(1)−Cu(1)−Cl(3)	87.82(7)
Cu(2)−Cl(4)	2.329(3)	Cl(1)#1−Cu(1)−Cl(3)	92.18(7)
Cu(2)−Cl(4)#2	2.329(3)	Cl(2)#1−Cu(1)−Cl(3)	92.15(8)
Cl(3)#2−Cu(2)−Cl(4)#2	90.43(9)	Cl(2)−Cu(1)−Cl(3)	87.85(8)
Cl(3)−Cu(2)−Cl(4)#2	89.57(9)	Cl(3)#2−Cu(2)−Cl(3)	180.00(13)
Cl(4)−Cu(2)−Cl(4)#2	180.000(1)	Cl(3)#2−Cu(2)−Cl(4)	89.57(9)
Cu(2)−Cl(3)−Cu(1)	165.62(11)	Cl(3)−Cu(2)−Cl(4)	90.43(9)

[a] Symmetry codes: #1 [$-x + 2$, $-y + 2$, $-z$]; #2 [$-x + 1$, $-y + 1$, $-z$].

Table 3. Hydrogen Bond Lengths (Å) and Bond Angles (deg) for Bis(dodecylammonium) Tetrachlorocuprate[a]

D−H···A	*d*(D−H)	*d*(H···A)	*d*(D···A)	<(DHA)
N(1)−H(1A)···Cl(4)	0.89	2.61	3.469(10)	163.1
N(1)−H(1A)···Cl(3)#2	0.89	2.89	3.428(9)	120.6
N(2)−H(2C)···Cl(2)	0.89	2.59	3.459(10)	165.2
N(2)−H(2C)···Cl(1)#1	0.89	2.90	3.423(10)	118.9
N(1)−H(1B)···Cl(3)#3	0.89	2.46	3.300(9)	157.9
N(1)−H(1C)···Cl(2)#4	0.89	2.42	3.259(9)	158.2
N(2)−H(2A)···Cl(4)#5	0.89	2.43	3.270(9)	157.7
N(2)−H(2B)···Cl(1)#3	0.89	2.46	3.296(10)	157.7
C(3)−H(3A)···Cl(2)#4	0.97	2.74	3.686(18)	165.7

[a] Symmetry code: #1 [$-x + 2$, $-y + 2$, $-z$]; #2 [$-x + 1$, $-y + 1$, $-z$]; #3 [$x - 1$, y, z]; #4 [$x - 1$, $y - 1$, z]; #5 [x, $y + 1$, z].

boiling and refluxing for 4 h. The final solution was laid aside, and several days later, a golden yellow transparent crystal was obtained. The crystal was recrystallized three times with anhydrous methyl alcohol and washed by ether three times. Finally, the sample was placed in a vacuum desiccator at $T =$ 300 K to dry in vacuum for 6 h. The final product was put into a weighing bottle and preserved in a desiccator. Theoretical contents of C, H, N, Cu, and Cl in the compound $(C_{12}H_{28}N)_2CuCl_4$(s) have been calculated to be 49.87 %, 9.76 %, 4.85 %, 10.99 %, and 24.53 %, respectively. Chemical and elemental analysis (model: PE-2400, Perkin-Elmer, USA) have shown that the practical contents of C, H, N, Cu, and Cl in the compound $(C_{12}H_{28}N)_2CuCl_4$(s) have been measured to be 49.85 %, 9.77 %, 4.83 %, 10.97 %, and 24.58 %, respectively. These results showed the purity of the sample prepared was > 0.995 in mass fraction.

X-ray Crystallography. A suitable single crystal (0.48 mm × 0.47 mm × 0.13 mm) of the complex was glued to fine glass fiber and then mounted on a Bruker Smart-1000 CCD diffractometer with Mo Kα radiation ($\lambda = 0.71073$ Å). The intensity data were collected in the $\varphi-\omega$ scan mode at $T = 298(2)$ K. The empirical absorption corrections were based on multiple scans. The structure was solved by the direct method and different Fourier syntheses, and all non-hydrogen atoms were refined anisotropically on F^2 by the full-matrix least-squares method. All calculations were performed with the program package SHELXTL.[9]

The crystal data and details of data collection and refinements for the complex are summarized in Table 1. The selected bond lengths and angles for the title compound are listed in Table 2. The hydrogen bond lengths and angles of the title compound are presented in Table 3. We have successfully applied for a CCDC (Cambridge Crystallographic Data Centre) number (777513) for the new synthesized complex.

Adiabatic Calorimetry. A precision automatic adiabatic calorimeter was used to measure heat capacities of the compound over the temperature range $78 \le (T/\mathrm{K}) \le 390$. The calorimeter was established in the Thermochemistry Laboratory of the College of Chemistry and Chemical Engineering, Liaocheng University, China. The principle and performance of the adiabatic calorimeter and the procedures of heat capacity measurements have been described in detail elsewhere.[7,10,11] Heat-capacity measurements were continuously and automatically carried out by means of the standard method of intermittently heating the sample and alternately measuring the temperature. Liquid nitrogen was used as the coolant. The heating rate and temperature increments were generally controlled at (0.1 to 0.4) K·min^{-1} and (1 to 3) K. The heating duration was 10 min, and the temperature drift rates of the sample cell measured in an equilibrium period were always kept within (10^{-3} to 10^{-4}) K·min^{-1} during the acquisition of all heat capacity data. The data of heat capacities and the corresponding equilibrium temperature have been corrected for heat exchange of the sample cell with its surroundings.[11] The reliability of the performance of the calorimeter was confirmed by the measurement of the heat capacities of the reference standard material (α-Al_2O_3) over the temperature range $77 \le (T/\mathrm{K}) \le 400$. Deviations of the experimental results from those of the smoothed curve lie within ± 0.20 %, while the uncertainty is ± 0.30 %, as compared with the values given by the former National Bureau of Standards[12] over the whole temperature range.

The sample mass used for the calorimetric measurement was 1.88343 g, which is equivalent to $3.258 \cdot 10^{-3}$ mol in terms of its molar mass, $M = 578.05$ g·mol^{-1}.

Differential Scanning Calorimetry (DSC). The DSC measurements were carried out in a Netzsch STA 449C made by Germary, Netzsch Instruments (Shanghai) Co., Ltd. with aluminum sample pans and empty material. The samples were scanned at a heating rate of 5 K·min^{-1} under the atmosphere of high purity nitrogen with a flow rate of 35 cm^3·min^{-1}. The mass of the sample used for the experiment was 2.950 mg.

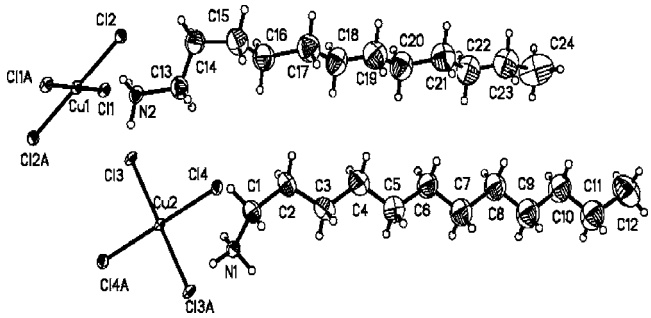

Figure 1. Molecular structure in the crystallographic independent unit of the compound bis(dodecylammonium) tetrachlorocuprate.

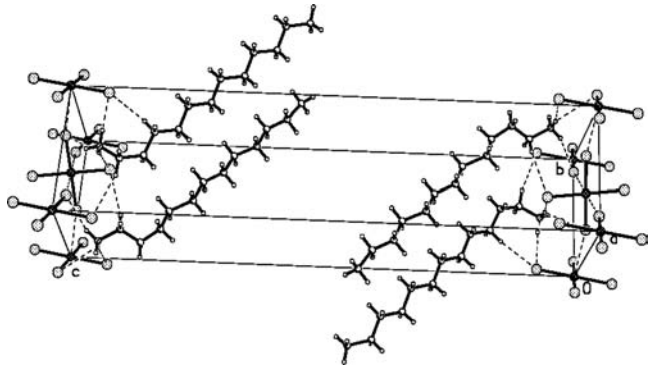

Figure 2. Packing of structure of the compound bis(dodecylammonium) tetrachlorocuprate in the unit cell.

Results and Discussion

Crystal Structure of Bis(dodecylammonium) Tetrachlorocuprate. It is found from Table 1 that the crystal structure of the compound is triclinic, the space group is *P*-1, and the unit cell dimensions are $a = 7.3357(6)$ Å, $b = 7.5884(7)$ Å, $c = 31.05(3)$ Å, $\alpha = 91.786(2)°$, $\beta = 90.9540(10)°$, $\gamma = 90.0600(10)°$, and $Z = 2$. The molecular structure in crystallographic independent units of bis(dodecylammonium) tetrachlorocuprate is plotted in Figure 1, and the packing of the cell structure is shown in Figure 2. From Figure 1 and Table 2, we can see that the steric configuration of $[CuCl_4]^{2-}$ in the coordination compound $(C_{12}H_{28}N)_2CuCl_4$ is almost square, and there are two types of monomeric $[CuCl_4]^{2-}$ molecules, which may be caused by the unequal bond lengths (Cu−Cl) and the bond angles (Cl−Cu−Cl) (see Table 2) in the crystallology aspect, but from the chemical composition, the monomeric $[Cu_1Cl_1Cl_{1A}Cl_2Cl_{2A}]^{2-}$ and the monomeric $[Cu_2Cl_3Cl_{3A}Cl_4Cl_{4A}]^{2-}$ units are equal (see Figure 1).

The monomeric $[CuCl_4]^{2-}$ moieties bind with the monomeric $[C_{12}H_{28}N]^+$ through several hydrogen bonds (see Table 3) including classical N−H···Cl hydrogen bonds and nonclassical C(3)−H(3A)···Cl(2) hydrogen bonds, with a bond length of C(3)···Cl(2) = 3.686(18) Å and bond angle C(3)−H(3A)···Cl(2) = 165.7°, symmetry code $[x - 1, y - 1, z]$. Because of the formation of the hydrogen bond, the polarity of two alkylammonium chains approach Cl atoms from two sides of $[CuCl_4]^{2-}$ moieties; this symmetric unit is stacked and forms a sandwich layered construction, and the unit $[CuCl_4]^{2-}$ resides in the "sandwich floor", giving rise to an infinite two-dimensional plane along the *ab*-plane (see Figure 3). On account of the binding action of hydrogen bonds, the molecule unit extends to a space supermolecule, which helps to establish a two-dimensional perovskite structure (see Figure 3). The results indicate that the hydrogen bonds play an important role in the stabilization of the whole structure.

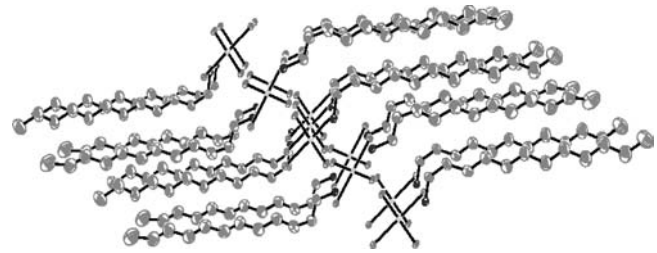

Figure 3. Laminated structure of the title compound. (All hydrogens were omitted for clarity.)

Lattice Potential Energy. The compound $(C_{12}H_{28}N)_2CuCl_4(s)$ can be regarded as a simple salt of the type of M_2X (charger ratio 1: 2), and the lattice potential energy of the compound can be obtained from the formula,[13]

$$U_{POT} = \gamma\left(\frac{\rho}{M_m}\right)^{1/3} + \delta \quad (1)$$

in which the constants of $\gamma = 8375.6$ kJ·mol^{-1}·cm and $\delta = -178.8$ kJ·mol^{-1} for M_2X (charge ratio 1:2) salts.

From the crystal structure information of Table 1, $\rho = 1.111$ g·cm^{-3}, $M_m = 578.05$ g·mol^{-1}, and the lattice potential energy of the compound $(C_{12}H_{25}NH_3)_2CuCl_4(s)$ is calculated to be $U_{POT} = 862.56$ kJ·mol^{-1}.

Low-Temperature Heat Capacities. The experimental results of low-temperature heat capacities are listed in Table 4 and plotted in Figure 4, which show that two obvious endothermic peaks appeared in the temperature range between $T =$ (311 and 333) K and $T =$ (333 and 340) K, respectively.

The experimental heat capacity values in the temperature range between $T = 78$ K and $T = 311$ K and between $T = 340$ K and $T = 390$ K were respectively fitted by means of the least-squares method, and two polynomial equations of the experimental molar heat capacities ($C_{p,m}$) versus reduced temperature (X), $X = f(T)$, have been obtained in the following:

(i) In the temperature range from $T =$ (78 to 311) K before the phase transition,

$$C_{p,m}/(J\cdot K^{-1}\cdot mol^{-1}) = 569.951 + 391.743X - 47.896X^2 + 1.518X^3 - 38.172X^4 + 29.072X^5 + 48.268X^6 \quad (2)$$

in which $X = (T/K - 194.5)/116.5$. The coefficient of determination for the fitting R^2 equals 1, in which 194.5 is half of the upper limit 311 K plus the lower limit 78 K, while 116.5 is half of the upper limit 311 K minus the lower limit 78 K. The reduced temperature (X) obtained using the method is placed between +1 and −1, and deviations of the smoothed heat capacities from the experimental values will become smaller and smaller with the increase of the power in the fitted polynomial equation according to statistical principles. The above eq 2 has an uncertainty of ± 0.3 %.

(ii) In the temperature range from $T =$ (340 to 390) K after the phase transition,

$$C_{p,m}/(J\cdot K^{-1}\cdot mol^{-1}) = 1040.176 + 79.397X - 1.608X^2 + 11.922X^3 - 0.609X^4 - 10.260X^5 \quad (3)$$

Table 4. Experimental Molar Heat Capacities of Series 1 of the Title Compound [$M((C_{12}H_{28}N)_2CuCl_4(s)) = 578.05\ g\cdot mol^{-1}$]

T	$C_{p,m}$	T	$C_{p,m}$	T	$C_{p,m}$
K	$J\cdot K^{-1}\cdot mol^{-1}$	K	$J\cdot K^{-1}\cdot mol^{-1}$	K	$J\cdot K^{-1}\cdot mol^{-1}$
78.387	111.80	171.32	489.04	284.43	849.10
79.914	118.05	173.94	498.63	287.42	858.43
82.326	128.00	176.46	507.04	290.35	868.32
84.737	139.69	179.26	518.48	293.37	877.08
87.069	150.40	183.21	531.78	296.55	891.68
89.319	160.03	185.82	540.74	298.99	903.94
91.490	170.39	189.61	552.87	301.93	911.53
94.705	179.63	192.29	563.53	304.78	924.38
95.809	186.83	195.15	573.38	307.64	939.56
97.921	197.20	197.99	582.60	310.58	962.92
99.930	206.49	200.69	592.18	313.43	992.70
102.02	216.14	203.55	600.09	316.33	1031.21
103.95	225.43	206.20	608.31	319.21	1099.83
105.96	232.58	209.00	618.02	322.12	1166.67
107.89	242.23	211.69	626.93	324.90	1557.67
109.82	250.45	214.24	635.62	327.16	5825.15
111.70	260.09	216.87	644.56	328.47	12075.74
113.60	265.45	219.49	652.38	329.57	10709.23
115.41	274.44	221.97	659.15	330.52	5459.73
117.21	280.32	224.45	667.49	332.68	1243.98
119.13	289.12	227.00	676.24	334.98	1542.24
121.96	299.76	229.62	682.51	337.53	3790.91
123.97	310.60	232.17	690.37	340.20	960.71
127.10	322.50	234.66	697.78	343.69	968.44
129.67	334.08	237.42	706.81	346.62	978.04
132.25	344.22	239.75	713.72	349.56	988.26
134.98	354.22	242.81	723.65	352.50	998.48
137.55	365.16	246.31	734.00	355.51	1009.93
140.20	375.60	249.85	744.21	358.53	1019.74
142.86	384.98	252.65	753.20	361.63	1029.96
145.44	395.22	255.40	760.63	364.65	1038.35
148.56	407.69	258.27	769.29	367.75	1047.74
150.62	415.89	261.11	777.83	370.76	1058.57
153.31	424.42	264.02	786.84	373.86	1069.40
155.87	433.11	266.94	795.42	376.88	1078.80
158.42	443.83	269.85	803.96	379.90	1088.82
161.04	452.35	272.70	813.67	383.00	1098.63
163.52	460.77	275.61	821.89	386.02	1107.62
166.14	470.35	278.53	831.56	389.03	1117.02
168.62	479.87	281.37	840.57		

in which $X = (T/K - 365)/25$. The coefficient of determination for the fitting R^2 equals 0.99987. The above eq 3 has an uncertainty of ± 0.2 %.

Molar Enthalpy and Entropy of the Solid−Solid Phase Transition. Six series of experiments in the phase transition region with different cooling rates for the sample were carried out so that the reversibility and repeatability of the phase transition of the sample were verified. The cooling rate of series 1 was about 15 $K\cdot min^{-1}$ (liquid nitrogen as the cooling agent), that of series 2 was about 2.5 $K\cdot min^{-1}$ (ice−water cooling), and that of series 3, 4, 5, and 6 was about 0.5 $K\cdot min^{-1}$ (natural cooling). The results of the six series of heat capacity measurements are plotted in the inlet to Figure 4. It can be seen from the inlet that there are some slight differences in heights and widths of peaks corresponding to each series of heat capacity measurements during the phase transition of the sample. However, the phase transition basically exhibited good reversibility and repeatability, and different cooling rates did not affect the experimental results. A close agreement in $C_{p,m}$ values of each series of repeated experiment was obtained. The area under the peak in the heat capacity curve is the enthalpy of the phase transition of all masses of the substances used in the calorimetric measurement. Namely, we can get the enthalpy of phase transition of the compound through integrating the area of the phase transition peak in the $C_{p,m}-T$ curve.

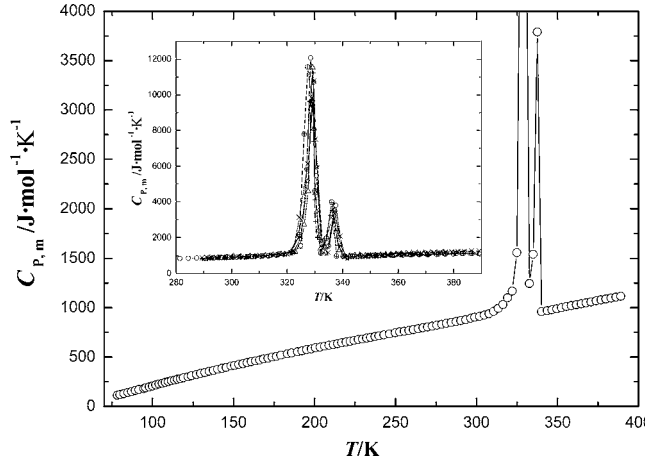

Figure 4. Curve of experimental molar heat capacities of the compound bis(dodecylammonium) tetrachlorocuprate with the temperature. ("○", "△", "☆", "+", "×", and "⊕" denote the first, second, third, fourth, fifth, and sixth series of measurements, respectively.)

The molar enthalpy of the phase transition ($\Delta_{trs}H_m$) in the $C_{p,m}-T$ curve was obtained from eq 4. The molar entropy ($\Delta_{trs}S_m$) of the phase transition was calculated with the following thermodynamic eq 5:[14]

$$\Delta_{trs}H_m = [Q - n\cdot\int_{T_i}^{T_{trs}} C_{P(i)}\,dT - n\cdot\int_{T_{trs}}^{T_f} C_{P(f)}\,dT - \int_{T_i}^{T_f} H_0\,dT]/n(kJ\cdot mol^{-1}) \quad (4)$$

$$\Delta_{trs}S_m = \Delta_{trs}H_m/T_{trs}(J\cdot K^{-1}\cdot mol^{-1}) \quad (5)$$

where T_i in eq 4 was the starting phase transition temperature, T_f was the finishing transition temperature, $C_{P(i)}$ was the heat capacity at the temperature T_i,$C_{P(f)}$ was the heat capacity at the temperature T_f, Q was the total heat quantity introduced to the calorimeter from temperature T_i to T_f, T_{trs} was the peak temperature of the phase transition of the sample, n was the

Table 5. Results of the Two Phase Transitions Obtained from Six Series of Repeated Experiments of Bis(dodecylammonium) Tetrachlorocuprate

	series 1	series 2	series 3	series 4	series 5	series 6	mean value
thermodynamic properties	x_i	x_i	x_i	x_i	x_i	x_i	$(\bar{x} \pm \sigma_a)^a$
$T_{trs,1}$/K	328.47	329.21	329.20	329.51	329.63	328.16	(329.03 ± 0.24)
$\Delta_{trs}H_{m,1}/(kJ\cdot mol^{-1})$	65.40	64.86	63.27	63.36	64.55	63.99	(64.24 ± 0.35)
$\Delta_{trs}S_{m,1}/(J\cdot K^{-1}\cdot mol^{-1})$	199.11	193.05	192.18	192.29	195.83	194.99	(194.57 ± 1.09)
$T_{trs,2}$/K	337.53	336.68	337.09	336.79	337.44	336.37	(336.98 ± 0.18)
$\Delta_{trs}H_{m,2}/(kJ\cdot mol^{-1})$	22.06	21.32	20.48	20.16	20.35	20.47	(20.81 ± 0.30)
$\Delta_{trs}S_{m,2}/(J\cdot K^{-1}\cdot mol^{-1})$	65.35	63.33	60.76	59.86	60.31	60.86	(61.75 ± 0.87)

[a] $\bar{x}$ is the mean value of a set of measurement results; $\sigma_a = [\sum_{i=1}^{n}(x - \bar{x})^2/n(n-1)]^{1/2}$, where n is the experimental number; x_i, a single value in a set of measurements.

Table 6. Smoothed Molar Heat Capacities and Thermodynamic Functions of the Complex Bis(dodecylammonium) Tetrachlorocuprate

T	$C_{p,m}$	$H_T - H_{298.15K}$	$S_T - S_{298.15K}$	$G_T - G_{298.15K}$
K	$J \cdot K^{-1} \cdot mol^{-1}$	$kJ \cdot mol^{-1}$	$J \cdot K^{-1} \cdot mol^{-1}$	$kJ \cdot mol^{-1}$
80	118.45	−116.79	−595.26	−69.17
85	140.34	−116.14	−587.43	−66.21
90	162.48	−115.39	−578.78	−63.30
95	184.70	−114.52	−569.39	−60.43
100	206.88	−113.54	−559.33	−57.61
105	228.89	−112.45	−548.70	−54.84
110	250.66	−111.25	−537.54	−52.12
115	272.13	−109.95	−525.92	−49.47
120	293.26	−108.53	−513.89	−46.87
125	314.03	−107.01	−501.51	−44.33
130	334.42	−105.39	−488.80	−41.85
135	354.43	−103.67	−475.82	−39.44
140	374.08	−101.85	−462.58	−37.09
145	393.38	−99.930	−449.12	−34.81
150	412.34	−97.916	−435.48	−32.59
155	431.00	−95.807	−421.65	−30.45
160	449.37	−93.606	−407.68	−28.38
165	467.48	−91.314	−393.58	−26.37
170	485.35	−88.932	−379.35	−24.44
175	503.00	−86.461	−365.02	−22.58
180	520.44	−83.902	−350.60	−20.79
185	537.69	−81.257	−336.10	−19.08
190	554.75	−78.526	−321.52	−17.44
195	571.63	−75.710	−306.89	−15.87
200	588.34	−72.810	−292.20	−14.37
205	604.87	−69.827	−277.46	−12.95
210	621.22	−66.761	−262.68	−11.60
215	637.38	−63.615	−247.87	−10.32
220	653.35	−60.388	−233.04	−9.120
225	669.13	−57.082	−218.18	−7.992
230	684.70	−53.697	−203.30	−6.937
235	700.09	−50.235	−188.42	−5.957
240	715.28	−46.696	−173.53	−5.050
245	730.30	−43.082	−158.63	−4.218
250	745.18	−39.394	−143.73	−3.460
255	759.95	−35.631	−128.84	−2.777
260	774.67	−31.794	−113.94	−2.169
265	789.42	−27.884	−99.052	−1.635
270	804.29	−23.900	−84.159	−1.177
275	819.40	−19.841	−69.261	−0.7937
280	834.91	−15.705	−54.354	−0.4859
285	851.00	−11.490	−39.428	−0.2533
290	867.90	−7.1934	−24.474	−0.09593
295	885.87	−2.8093	−9.4772	−0.01354
298.15	897.87	0	0	0
300	905.21	1.6679	5.5789	−0.005782
305	926.29	6.2460	20.715	−0.07211
310	949.54	10.935	35.957	−0.2118
315	phase change			
320	phase change			
325	phase change			
330	phase change			
335	phase change			
340	956.90	99.347	303.48	−3.837
345	972.64	104.17	317.56	−5.390
350	990.10	109.08	331.68	−7.013
355	1007.5	114.07	345.85	−8.707
360	1024.1	119.15	360.06	−10.47
365	1040.2	124.31	374.30	−12.31
370	1056.1	129.55	388.56	−14.21
375	1072.3	134.87	402.84	−16.19
380	1088.9	140.27	417.15	−18.24
385	1105.2	145.76	431.49	−20.36
390	1119.0	151.32	445.85	−22.56

mole number of the sample, and H_0 was the heat capacity of the empty sample cell. The values of Q and H_0 were calculated with the program stored in the computer linked with the adiabatic calorimetric system, and printed along with experimental results of heat capacities. The results of T_{trs}(K), $\Delta_{trs}H_m$ ($kJ \cdot mol^{-1}$), $\Delta_{trs}S_m$ ($J \cdot K^{-1} \cdot mol^{-1}$), and their average values obtained from every series of repeated experiment are listed in Table 5. It can be seen from Table 5 for the same sample that the two phase enthalpies of series 1 are both higher than the other five series, which is possibly ascribed to better crystallization of the sample in the first measurement.

For $(C_{12}H_{28}N)_2CuCl_4$, two structural phase changes are presented above 300 K. On increasing temperature, two continuous phase transitions appear. Kang et al.[3] studied the phase transition mechanism of this compound by infrared spectra: with the increase of temperature, the hydrogen bonds became weakened, which made constraints between alkylammonium chains, and $[CuCl_4]^{2-}$ became weakened. The partial disorder of alkylammonium chains occurred together with the reversal of polar NH_3 groups; thus, the structure of the molecule is transformed, and another kind of free and partly disordered solid phase is formed in the first phase transition. In the second phase transition, further conformational changes of the hydrocarbon part are dominant. When the second phase transition is over, the whole solid phase is in complete disorder. After that, the temperature progressively increases, and N−H stretching vibration absorption peaks are no longer changed significantly, which means that solid−solid phase changes have finished, and the stable structure of a new solid phase is maintained until the solid−liquid phase change occurs. The phase transition mechanism of this compound is analogous to many other (n-$C_nH_{2n+1}NH_3)_2MX_4$ compounds.[15−18]

Smoothed Heat Capacities and Thermodynamic Functions of the Compound. The smoothed molar heat capacities and thermodynamic functions were calculated based on the fitted polynomial equations of the heat capacities as a function of the reduced temperature (X) according to the following thermodynamic equations,

$$(H_T - H_{298.15}) = \int_{298.15}^{T} C_{p,m}\,dT \tag{6}$$

$$(S_T - S_{298.15}) = \int_{298.15}^{T} C_{p,m} \cdot T^{-1}\,dT \tag{7}$$

$$(G_T - G_{298.15}) = \int_{298.15}^{T} C_{p,m}\,dT - T \cdot \int_{298.15}^{T} C_{p,m} \cdot T^{-1}\,dT \tag{8}$$

The polynomial fitted values of the molar heat capacities and fundamental thermodynamic functions of the sample relative to the standard reference temperature of 298.15 K are tabulated in Table 6 at the intervals of 5 K.

Results of DSC Analysis of the Compound. The results of DSC analysis for the title compound are shown in Figure 5. It can be seen from Figure 5 that there are three endothermic processes in the temperature range from (310 to 570) K. The first two peaks on the DSC curve are in accordance with the two phase transition peaks appearing on the $C_{p,m}-T$ curve, and the third is a melting peak. The comparison of the temperatures and molar enthalpies of the phase transitions by DSC and precision automatic adiabatic calorimetry (PAAC) are shown in Table 7, and the results show that the molar enthalpy of the phase transition of $(C_{12}H_{28}N)_2CuCl_4$(s) obtained by a precision automatic adiabatic calorimeter is a little higher than that determined by Netzsch STA 449C DSC and leads to a difference of 11.03 $kJ \cdot mol^{-1}$ for the first phase change peak and 1.9 $kJ \cdot mol^{-1}$ for the second phase change peak for the same sample, and the phase transition temperatures are not very close to each other, which is possibly ascribed to the fine measuring performance of the adiabatic calorimeter with high accuracy and precision. Our results for the phase transition enthalpies are larger than that determined by a Rigaku TAS-100 DSC in 1993[3]

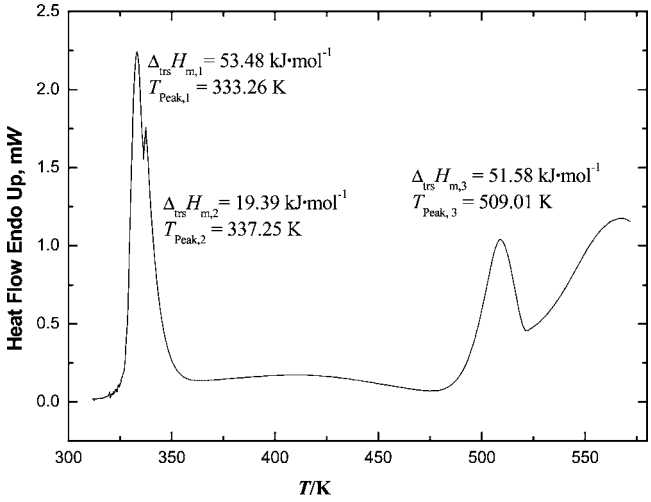

Figure 5. Curve of DSC for bis(dodecylammonium) tetrachlorocuprate with a scanning rate of 5 K·min^{-1}.

Table 7. Comparison of Temperature and Molar Enthalpy of the Phase Transitions Obtained by Different Calorimetry Techniques

	T_{trs}	$\Delta_{trs}H_m$
calorimeter	K	kJ·mol^{-1}
First Phase Transition Process		
Rigaku TAS-100 DSC[3]	327.9	(39.71 ± 0.15)
Perkin-Elmer DSC-7[4]	325.69	34.16
Netzsch STA 449C DSC[a]	333.26	53.48
PAAC[b]	(329.03 ± 0.24)	(64.24 ± 0.35)
Second Phase Transition Process		
Rigaku TAS-100 DSC[3]	335.7	(8.33 ± 0.09)
Perkin-Elmer DSC-7[4]	332.22	6.39
Netzsch STA 449C DSC	337.25	19.39
PAAC	(336.98 ± 0.18)	(20.81 ± 0.30)

[a] Differential scanning calorimeter. [b] Precision automatic adiabatic calorimeter.

and Perkin-Elmer DSC-7 in 1998,[4] possibly ascribed to the higher purity and better crystallization of the sample in our work.

Conclusions

This paper mainly reported the crystal structure, lattice potential energy, and low temperature heat capacities in the temperature region from (78 to 390) K. Two solid-to-solid phase transitions were found in the $C_{p,m}-T$ curve. The molar enthalpies and molar entropies of the two solid−solid phase changes were obtained according to thermodynamic equations. The relevant thermodynamic properties of the solid state compound bis-(dodecylammonium) tetrachlorocuprate were determined.

Literature Cited

(1) Li, J. L.; Xue, P.; Ding, W. Y.; Han, J. M.; Sun, G. L. Micro-encapsulated Paraffin/high-density Polyethylene/wood four Composite as Form-stable Phase Change Material for Thermal Energy Storage. *Sol. Energy Mater. Sol. Cells* **2009**, *93*, 1761–1767.

(2) Nomura, T.; Okinaka, N.; Akiyama, T. Impregnation of Porous Material with Phase Change Material for Thermal Energy Storage. *Mater. Chem. Phys.* **2009**, *115*, 846–850.

(3) Kang, J. K.; Choy, J. H.; Madeleine, R. L. Phase Transition Behavior in the Perovskite-type Layer Compound (n-$C_{12}H_{25}NH_3)_2CuCl_4$. *J. Phys. Chem. Solids* **1993**, *54* (11), 1567–1577.

(4) Li, W. P.; Zhang, D. S.; Zhang, T. P.; Wang, T. Z.; Ruan, D. S.; Xing, D. Q.; Li, H. B. Study of Solid-Solid Phase Change of (n-$C_nH_{2n+1}NH_3)_2MCl_4$ for Thermal Energy Storage. *Thermochim. Acta* **1999**, *326*, 183–186.

(5) Wu, K. Z.; Zhang, J. J.; Liu, X. D. Subsolidus Phase Diagram of Binary System of Thermotropic Phase Transitions Compounds (n-$C_nH_{2n+1}NH_3)_2MnCl_4$ (n = 12, 14, 16). *Thermochim. Acta* **2009**, *483*, 55–57.

(6) Arend, H.; Huber, W. Layer Perovskites of the $(C_nH_{2n+1}NH_3)_2MX_4$ and $NH_3(CH_2)$ $m NH_3MX_4$ Families with M = Cd, Cu, Fe, Mn or Pd and X = Cl or Br: Importance, Solubilities and Simple Growth Techniques. *J. Cryst. Growth* **1978**, *43*, 213–223.

(7) Tan, Z. C.; Shi, Q.; Liu, B. P.; Zhang, H. T. A Fully Automated Adiabatic Calorimeter for Heat Capacity Measurement between 80 and 400 K. *J. Therm. Anal. Calorim.* **2008**, *92* (2), 367–374.

(8) White, M. A. Characterization of Solid-Solid Phase Transitions: Differential Scanning Calorimetry vs. Adiabatic Calorimetry. *Thermochim. Acta* **1984**, *74* (1−3), 55–62.

(9) Sheldrick, G. M. A Short History of SHELX. *Acta Crystallogr.* **2008**, *A64*, 112–122.

(10) Kong, Y. X.; Di, Y. Y.; Yang, W. W.; Zhang, D. D.; Tan, Z. C. Low-Temprature Heat Capacity and Thermodynamic Properties of Triaquabenzoatocalcium Monobenzoate [Ca(Ben)$(H_2O)_3$](Ben)(s) (Ben = Benzoate). *J. Chem. Eng. Data* **2009**, *54*, 2256–2262.

(11) Tan, Z. C.; Liu, B. P.; Yan, J. B.; Sun, L. X. A Fully Automated Adiabatic Calorimeter Workable between 80 and 400 K. *J. Comput. Appl. Chem.* **2003**, *20* (3), 264–268.

(12) Ditmars, D. A.; Ishiha, S.; Chang, S. S.; Bernstein, G. Enthalpy and Heat-Capacity Standard Reference Material: Synthetic Sapphire (α-Al_2O_3) from 10 to 2250 K. *J. Res. Natl. Bur. Stand.* **1982**, *87* (2), 159–163.

(13) Jenkins, H. D. B.; Tudela, D.; Glasser, L. Lattice Potential Energy Estimation for Complex Ionic Salts from Density Measurements. *Inorg. Chem.* **2002**, *41*, 2364–2367.

(14) Di, Y. Y.; Tan, Z. C.; Wu, X. M.; Meng, S. H.; Qu, S. S. Heat Capacity and Thermochemical Study of Trifluoroacetamide ($C_2H_2F_3NO$). *Thermochim. Acta* **2000**, *356*, 143–151.

(15) Lee, C. H.; Lee, K. W.; Lee, C. E. Quasi-two-dimensional Magnetism in $(C_nH_{2n+1}NH_3)_2CuCl_4$ Studied by Electron Paramagnetic Resonance. *Curr. Appl. Phys.* **2003**, *3*, 477–479.

(16) Guo, N.; Wang, W. Infrared Spectroscopic Study of Mechanism of Phase Transition in Dodecylammonium Tetrachlorozincate. *Chin. J. Appl. Chem.* **1994**, *11* (4), 25–30; in Chinese.

(17) Zuo, P.; Wu, K. Z.; Cui, W. Z.; Liu, X. D. Synthesis Characterization of Bis(n-decylammonium) Tetrachlorometallates(II). *J. Hebei Normal Univ. (Nat. Sci. Ed.)* **2002**, *26* (1), 53–55; in Chinese.

(18) Guo, N.; Wang, W.; Zeng, G. F.; Xi, S. Q. Raman Spectroscopic Study of Crystal Phase Transition in Bis(n-undecylammonium) Tetrachlorozincate. *Acta Chim. Sin.* **1994**, *52*, 705–710; in Chinese.

Received for review June 30, 2010. Accepted October 30, 2010. This work was financially supported by the National Natural Science Foundation of China under the contract NSFC No. 20673050 and 20973089.

JE100699G